

## PROCESSING IN HAIL SUPPRESSION SYSTEM WEATHER RADAR SIGNAL AND DATA

Predrag Vuković, Dejan Rančić  
Aleksandar Kostić, Bratislav Milovanović, Predrag Eterica,

**Abstract.** The weather radar signal and data processing of the automated hail suppression system is described in this paper. The created system increases efficiency of the radar center by applying automation of process from collecting radar information about clouds to launching rocket with seeding material. The signal processing algorithms and the architecture of the system as well as software organization for real time DSP (Digital Signal Processing) of weather radar echo are presented and discussed, with emphasis as to problem of estimation of mean reflected power from meteorological targets. The specialized information system based on GIS (Geographical Information System) technology and object oriented paradigm is developed as a subsystem. Also, the antenna moving control subsystem. The automated hail suppression system is designed for a wide range of applications such as: hail suppression activities, meteorological research, precipitation measurements and short-term forecast.

### 1. Introduction

Weather radars have been used since the 1950s for qualitative assessment of meteorological phenomena measurable by radars. Research has been directed towards providing short-term forecasting and hydrological data in a clear and unambiguous manner. There are three main applications of this information: storm warning and hail suppression activities are the first and most frequent applications of weather radars. The second is short-term forecasting and the third application is in hydrology, involving the measurement of water content reaching the ground and control of the water resources thereafter.

---

Manuscript received October 17, 1997.  
A version of this paper was presented at the third Conference Telecommunications in Modern Satellite and Cable Services, TELSIKS'97, October 1997, Niš, Yugoslavia.  
M.S. A. Kostić is with Military Technical Institute, Katanićeva 13, Beograd, Yugoslavia. The other authors are with Faculty of Electronic Engineering, University of Niš, Beogradska 14, Niš, Yugoslavia.

The system described in this paper is designed for the first application but it can be extended for the remaining two. Hail suppression system is very complex and very large one. Radar center automation system has been under development for some time at the Faculty of Electronic engineering in Ni under support of Hydrometeorological Service of Serbia and Ministry of science and technology of republic of Serbia.

Increasing efficiency of hail suppression system means to introduce the seeding material in precise defined volume of hail cells in clouds by the rockets launched from the ground. For this purpose, it is necessary to have very accurate measurements of cloud radar reflectivity, the seeding zones geometrical characteristics determination, tracking and prediction of their positions. According to prepared meteorological and technical criteria and certain meteorological seeding methods, the information subsystem, as a part of the realized automated system, makes the decision and selects the hail suppression stations (HSS), to launch the rockets with maximum calculated efficiency, separately. The identification numbers, rocket launching azimuth and elevation data, separately for all HSS, and corresponding timing, follows selected HSS by the automated system. The operator who coordinates hail suppression activities makes the final decision about launching the rocket among the selected HSS according to given efficiencies.

Methodology of hail suppression activities needs special requirements in regard of processing weather echo power and shape of an antenna volume scan. For this purpose, the following has been developed:

- hail cells in CP (cumulonimbus) clouds analysis on the basis of their reflectivity as described in Section 2. Following the operator's requirements, the system is able to perform very precise analysis up to the spatial resolution level determined by the antenna revolution speed and pulse repetition rate in the angular domain and the A/D converter sampling rate in the range domain. Maximum applied sampling rate is 4 MHz corresponding to the 37.5m range resolution.
- Time, angle and range averaging of radar echoes from distributed targets (clouds) has been implemented in the system in different degrees, according to modes of operations, through the moving window integration-adaptable.
- Because of getting the radar picture without uncovered zone in the analyzed cloud's cell, the antenna speed is automatically adaptable from 0.1 to 6 rpm (it depends on the radar servo system sensitivity), according to the applied A/D converter sampling rate.
- Volume sectorial scans of the radar antenna. The limits of the sector, in azimuth and elevation directions, are automatically adaptable and

determined by geometrical characteristics of cloud cells at a certain reflectivity level selected by operator.

## 2. Automated hail suppression system description

The new automated hail suppression radar center (Fig.1.), [12], consists of the MITSUBISHI RC-34A radar, main workstation, two additional workstations and intelligent microwave link. The workstations are connected by Ethernet LAN. The effective, flexible, modern solution of the radar signal processing is implemented by connecting an additional hardware to a PC motherboard. The additional hardware transforms the system into a very powerful one for digital signal processing. Three additional cards have been installed into the main workstation: A/D converter for radar log-video signal, DSP, containing two digital signal processors (TMS320C040) and A/D, D/A and digital I/O general purpose card. The high speed of the A/D converter and ability of external sampling control enables a dynamic change of the sampling rate, i.e. range resolution of reflected radar signals. DSP card processes the digitized radar signals (three-dimensional polar volume data) in real time [9] and stores the calculated data (volumetric data in Cartesian coordinate system) into the RAM of the main workstation for various meteorological products generation.

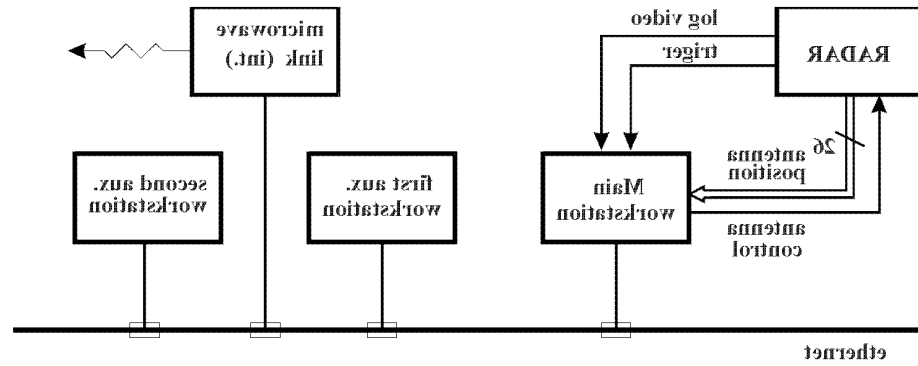


Figure 1. New automated hail suppression radar center.

The intelligent microwave communication link is also a part of the system responsible for data transmission between radar and command center as well as between nearest radar centers.

The main workstation (Fig.2.) performs numerous tasks, [8]. Some of them are: digitization of radar signals, compensation for attenuation

caused by electromagnetic waves propagation through the atmosphere, comparison with certain thresholds, integration and averaging in time, angle and range domain. Then, transformation from polar to Cartesian coordinates [13], memory mapping and storing data into the RAM of the main workstation, transfer of one radar sweep processed data to host memory, antenna scan regime control [12], man-machine interfacing [2], generating meteorological products, etc.

### 3. Signal processing

In radar meteorology, the average of the weather echo power is used in the computation of reflectivity, liquid water content, rainfall rate, etc. [6], [1], [4]. Typical receivers used in radars are linear, quadrature and logarithmic type. Any of them can be used to estimate the power return from distributed scatterers, such as clouds, but owing to the large dynamic range of meteorological signals [6], the logarithmic receiver is commonly employed. In MITSUBISHI RC-34A radar, too.

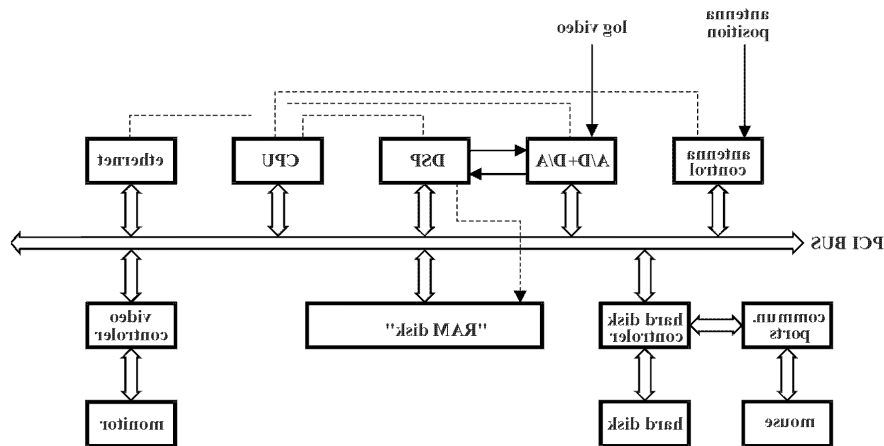


Figure 3. The main workstation configuration.

Estimates of mean reflected power  $P_0$  are obtained from  $N$  sample averages of receiver output signals (assumed to be independent). The estimation problem is complicated due to the fact that the input-output transfer function  $Q_s = q(P_s)$  is nonlinear (except for the quadratic type). Thus, the computationally efficient first estimate  $\hat{Q}_N$  of the reflected power is obtained

$$(1) \quad \hat{Q}_N = \frac{1}{N} \sum_{i=1}^N Q_i$$

and then the input power estimate  $\hat{P}_N$  is computed,

$$(2) \quad \hat{P}_N = \varrho^{-1}(\hat{Q}_N).$$

It is shown that under assumption of Rayleigh distributed receiver input envelope, i.e.

$$(3) \quad p(A) = \frac{2A}{P_0} \exp\left(-\frac{A}{P_0}\right),$$

where  $A$  is the amplitude, estimate  $\hat{P}_N$  is biased by constant factor (in dB) compared to unbiased one which can be obtained by averaging  $\varrho^{-1}(\hat{Q}_i)$ , which is much more time and memory consuming [10].

In the systems such as weather radars, either block averaging or first-order digital filters have been employed. A weighted window is practical to implement and also provides a continuous estimate of the mean value [10]. Block averaging integration is not strictly continuous. In system that is taken into consideration, the sweep-to-sweep and range averaging is performed by moving window integration.

Since the signal at the detectors, output is proportional to the input power, the difference equation for the estimate  $\hat{P}_N = Q_N$  at the  $N$ -th iteration is

$$(4) \quad \hat{Q}_N = \hat{Q}_{N-1} + \frac{1}{N} Q_N - \frac{1}{N} Q_{N-N}.$$

Assuming an initial condition  $Q_0 = 0$ , the filters' output can be expressed in term of  $Q_N$  as

$$(5) \quad \hat{Q}_N = \frac{1}{N} \sum_{i=1}^N Q_{i+N-N}.$$

For the assumed Rayleigh input amplitude distribution (3), the distribution of input power is exponential. It is shown [10] that the expected value and the standard deviation of  $\hat{P}_N$  for logarithmic receiver-detector are:

$$(6) \quad E(\hat{P}_N) = P_0 \left(1 + \frac{1}{N}\right),$$

$$(7) \quad \sigma(\hat{P}_N) = \sqrt{P_0^2 \left(1 + \frac{2}{N}\right) - \left(P_0 \left(1 + \frac{1}{N}\right)\right)^2}.$$

respectively.  $\gamma$  is the gamma function. On the contrary to square-law receiver, that is an unbiased estimator, the logarithmic receiver introduce a bias which is a function of  $N_i$ , as can be seen from the expression for the expected value of  $\hat{V}_i$ .

Implementation of the algorithm was made for the case of a Gaussian-shaped Doppler spectrum, a Gaussian-shaped antenna pattern and a rectangularly shaped transmitted pulse. An infinite bandwidth receiver, stationarity and homogeneity are assumed, too.

It is essential to determine the accuracy of mean intensity estimates from weather echoes. When independent radar echo data are averaged, the variance of the mean intensity estimate is inversely proportional to the number of samples [2]. This reduction in variance may be used as a measure of precision of the mean estimate. Also, the number of independent samples used to make the mean intensity estimate may be used as a measure of precision of the mean estimate. When dependent radar data samples are averaged, we use as a measure of precision either the variance reduction or the equivalent number  $N_i$  of independent samples. It means that  $N_i$  associated with a mean intensity estimate is defined as the ratio of the receiver signal variance to the variance of the mean intensity estimate [6], [18].

$$(8) \quad N_i = \frac{\sigma_{\hat{V}_i}^2}{\sigma_{V_i}^2}$$

where  $\hat{Q}$  is output sample and  $\hat{Q}$  is mean output estimates.

In a typical pulse radar system, echo signals are sampled at regularly spaced instants (i.e. regularly spaced slant range points) while antenna axis changes angular position at a constant rate. Under these conditions, time and range can be considered as independent variables. Angle sampling is then related to time in terms of a constant rotation rate  $\alpha$ . The correlation function for angle and time at one range is compiled as follows:

$$(9) \quad \rho(\alpha, \tau) = \exp \left[ \frac{-\tau^2}{2(\sigma_\tau^2)^2} \right]$$

$$(10) \quad \rho(\tau) = \left( \frac{\vartheta}{\theta_1} \right)^2 + \rho(\tau) e^{-\tau^2}$$

where  $\rho(\alpha, \tau)$  is the normalized correlation function for angle and time,  $\theta_1$  is the correlation time scale,  $\theta_1$  is the antenna beamwidth and  $\vartheta = \ln 2$  [18].

One needs only to compute values of  $\tau_s$  and obtain  $N_s$  for combined time and angle sampling from the next equation [18].

$$(11) \quad \left[ \left( \frac{K l_{\tau}}{\tau_s} \right)^{-m} \exp(-\tau_s N^m) - N - \sum_{m=1}^{\infty} \sum_{k=1}^{N-1} \frac{1}{\tau_s} + \frac{1}{N} \right] = N_s^{-1} \log^{-1} N_s$$

where subscript log stands for logarithmic receiver,  $N$  is the number of discrete samples spaced  $\tau_s$  seconds apart.

To include range with the combined time and angle sampling,  $N_s$  would be the number computed (for time-angle) multiplied by the number of independent samples in range. For  $N$  discrete range samples spaced a distance  $l_{\tau}$ ,  $N_s$  is [18]:

$$(12) \quad \left. \begin{aligned} \frac{1}{N_s} &= \left\{ \frac{1}{N} + \sum_{m=1}^{\infty} \sum_{k=1}^K \frac{1}{N^{\tau_s k}} (N - k)^{m-1} \left( 1 - \left( \frac{K l_{\tau}}{D_0} \right)^{2m} \right) \right\}^{-1} \\ \frac{D_0}{l_{\tau}} &\geq K^m \end{aligned} \right\} \quad \text{if } \tau_s < D_0$$

where  $D_0$  is the pulse volume length.

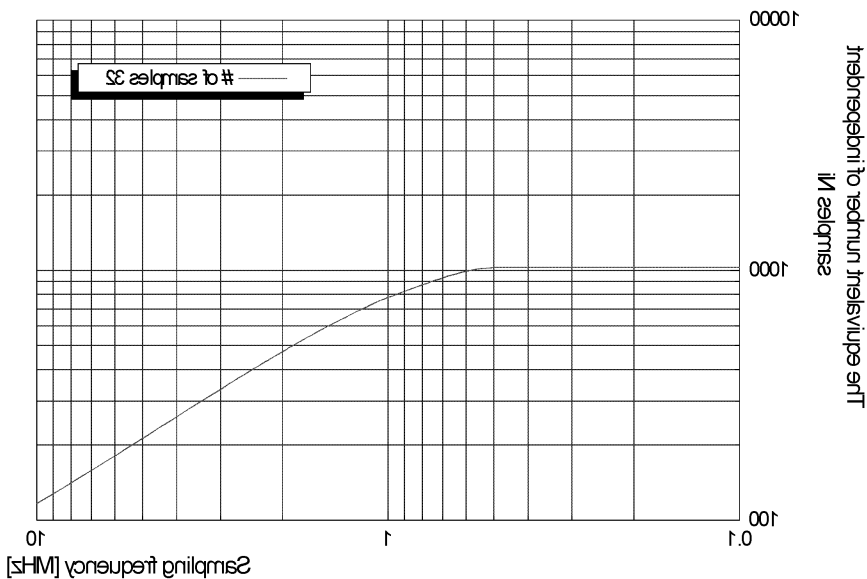


Figure 3. Equivalent number of independent samples for applied 32 discrete samples of the logarithmic receiver versus sampling frequency.

#### 4. Calibration of radar

To obtain the desired accuracy in radar reflectivity estimates for digital-  
 relative use it is necessary to verify a sufficient system stability and to get real  
 parameters that depend on transmitter power, sensitivity of the receiver,  
 wavelength, antenna properties and so on, in order to correct measurements  
 and possibly  $\Delta$ - $R$  relationship [3], [10].

From the second order polynomial regression of the measured radar cal-  
 ibration curve, one can get its coefficients. Figure 4 shows the calibration  
 curve belonging to weather radar MITSUBISHI RC-34A installed on the  
 hail suppression radar center Kamenniki Vis near Nis. These coefficients in  
 conjunction with the parameters of the radar included in  $G_2$  and compen-  
 sation for attenuation due to distance of the observed distributed scatterers  
 (an analogue to sensitivity Time Control in classic radar designs) transform  
 their reflectivity in meteorological used measure- $dBZ$  [14].

$$10 \log Z [dBZ] = A_1 (k_{tU^b})^2 + A_2 k_{tU^b} + A_3 + G_{2dB} \quad (13)$$

$$+ 20 \log v \Delta r + 2k \frac{n \Delta r}{1000}$$

where:

- $A_1, A_2$  and  $A_3$  - the calibration coefficients of radar,
- $k_{tU^b}$  - the analog to digital transformation coefficient,
- $U^b$  - the estimated receiver output sample in digital form,
- $\Delta r$  - range bin length,
- $v$  range bin ordinal number,
- $k$  - the attenuation coefficient in the atmosphere, and

$$G_2 = \frac{\pi^2}{2^{10} \ln 2} \frac{P_t h^2}{\lambda^2} |K|^2 G_2 \theta \phi \quad (14)$$

where are:  $P_t$  - transmitter power,  $h$  - pulse length,  $\lambda$  - wavelength,  $G_2$  -  
 antenna gain,  $\theta, \phi$  - beamwidths,  $v$  - losses and  $|K|^2$  - the refractive index.

Influence of the receiver thermal noise on the meteorological product dis-  
 play is limited by the comparing averaged signal level with threshold ob-  
 tained by well-known CA-CFAR algorithm [17], slightly modified, applied  
 on periodically estimated mean noise power. Namely, noise samples are  
 taken from a few gates belonging to the time interval beyond maximum  
 range of radar, under assumption that the time interval is clear of clutter  
 and meteorological targets. Weighted mean value of the noise samples de-  
 termines the threshold according to the CFAR algorithm. Only the signals  
 above threshold undergo  $v_2$  compensation [1].



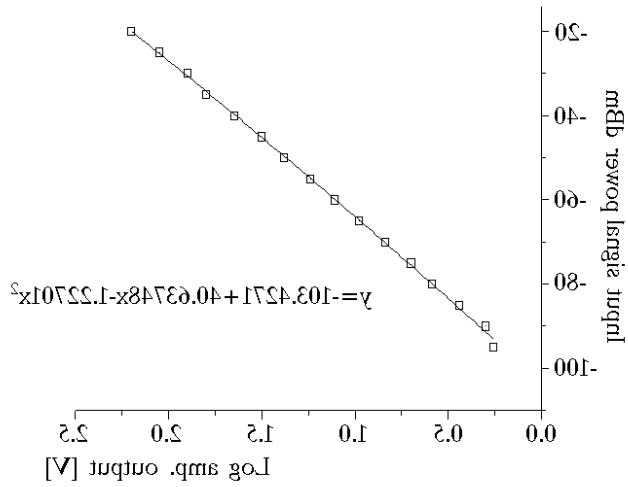


Figure 4. MITSUBISHI RC-34A Calibration curve (Radar Center Vis).

## 5. Real time software

This section describes implementation of real time part of main workstation software in brief.

Besides the intended functionality, software organization of the main workstation is strongly influenced by hardware architecture and operating system issues. As already mentioned, the main workstation is based on PC platform running under Windows, its operating system. Hardware specifics of DSP, A/D and digital I/O cards impose some constraints and partly determine real-time software structure, especially disposition of its components at processors. Also, various tasks performed by the main workstation application request different priorities and/or service-time delay boundaries, and have a wide range of execution times – characteristics that strongly suggest application of decoupling even parts of the same task which are distributed among 2 DSPs and host processor.

Real time software that performs tasks listed in section 1, consists of three main parts: DSP0 program, DSP1 program and host processor program. DSP0 and DSP1 programs are downloaded at the beginning of the host application software initialization, using the DSP's system routines. Next phase of initialization commences after DSP programs start-up and its purpose is to establish memory buffer through which radar picture is

transferred from DSPs to host. Due to relatively high and constant required data throughput of about 2 MB/s, slow data transferring routines from DSP card device driver are useless, and the only satisfactory solution is to perform direct data transfer to host memory by means of DSP card's PCI controller in bus master mode. However, serious problem to this conceptually simple idea is posed by the Windows' 95 implementation of memory management, reflected in the fact that there is no simple and generally predictable correspondence between virtual memory addresses user application program sees and works with, and physical addresses corresponding to them. Size of elementary memory chunk in Windows' 95 OS is 4 kB implying that 12 least significant address bits are the same in virtual and physical address, while mapping of 20 higher order bits is defined by the tables managed by operating system kernel executing at 0-th privilege level, that are completely invisible to the user application running at level 3 of privilege. An elegant solution to this problem is to let the host processor reserve memory space for the buffer and put some unenumerated markers at the 4 kB boundaries, and start scanning of the memory by the DSP in bus master regime (Fig. 8). By the time when all markers have been found, DSP has maintained table of starting addresses of host memory blocks belonging to buffer. In order to prevent random occurrence of marker somewhere in memory, actual procedure is performed in two steps: DSP memory scan and markers modification, in the first, and host verification that markers are modified in expected way, in the second step.

After initialization, system starts acquisition and processing of radar echoes [8]. Steps involved in processing of one radar pulse are outlined in Fig. 9.

Radar trigger pulse ( $trig_i$ ) starts RF pulse emission and synchronizes both radar and automated hail suppression subsystem. It starts acquisition of receiver signal samples block performed by A/D card as well as acquisition of current antenna position accomplished through steps ① – ③. At the instant ① trigger interrupts DSP0 which in turn issues interrupt to host processor ( $int_{c_i}$ ). During interrupt processing host reads antenna coordinates through digital I/O card and transfers them through waveform register of DSP card's PCI controller. Writing to this register issues interrupt to DSP 0 (③) which accepts data and associates them to data belonging to sweep  $i$ .

A/D converter outputs 12-bit samples to 1024 words long A/D card FIFO register. As FIFO is 16-bit wide, samples are sign-extended. After the FIFO is filled, TMS communication port<sup>1</sup> controller starts transmission

<sup>1</sup>Digital signal processor TMS320C040 has six 8-bit wide, 20 MB/s asynchronous communication ports that enable fast I/O and networking.

to one of DSP 0 communication ports (4) which lasts as long as FIFO holds more than 512 samples. Hence, FIFO introduces delay of  $512 T_s$  ( $T_s -$  sampling period), which is in worst case (for the minimum sampling rate  $f_{s_{min}} = 300\text{kHz}$ ) about 1.7ms. Samples are received by DSP 0 component attached internally to one of six channels of DMA coprocessor which packs pairs of 16 bit samples in 32-bit words and stores them in one of two input samples buffers. After transmission of programmed number of samples DMA stops and issues interrupt to DSP 0 informing it that new sweep data is ready for processing (5).

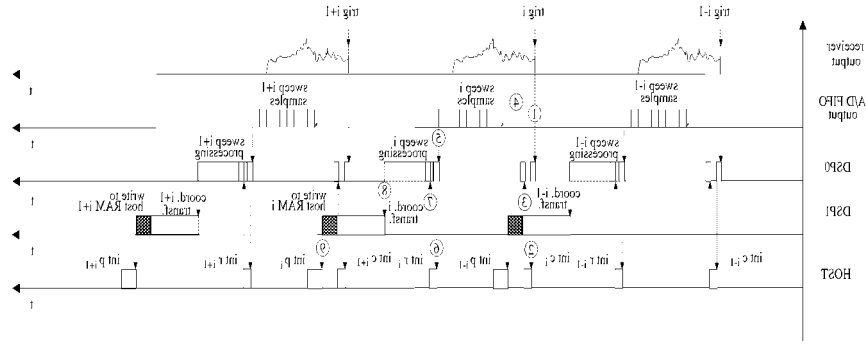


Figure 5. Time sequences of echo signals processing.

Interrupt servicing routine (ISR) interrupts host processor ( $int\ r_i$ ,  $\dagger$ ) and in case DSP 0 has finished sweep  $i - 1$  processing, performs buffer switching, so that DMA receiving buffer and DSP 0 processing buffer are exchanged (Fig. 6). At exit, ISR sends signal to main loop and so initiates new cycle of processing. Host ISR servicing  $int\ r_i$  resets FIFO and reinitializes A/D card preparing it for new echo acquisition, interrupting DSP 0 (5) before exiting. Having received this interrupt, DSP 0 reinitializes DMA coprocessor.

After unpacking, samples from processing buffer are input to the sweep-to-sweep integration filter whose output is fed to a range integration filter. Its output is compared to CFAR threshold obtained through procedure mentioned in previous section. Samples above the threshold are corrected for  $r_s$  and atmospheric attenuation and finally converted from dBm to dBz units.

Processed samples are stored in one of the four blocks of circular buffer (sl and s4), implemented in the DSP global memory (Fig. 7). The length of data blocks is matched to the number of samples corresponding to sweep maximum resolution. In addition to a length of used block, slot header

stored previous samples in circular buffer slot also contains azimuth and elevation of the radar antenna.

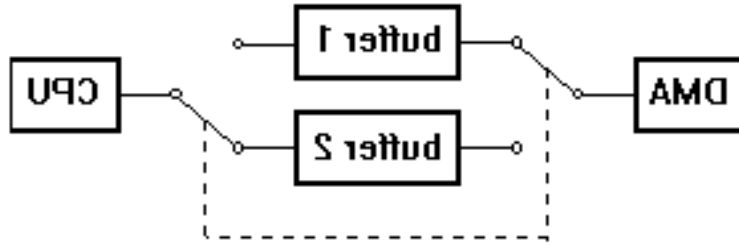


Figure 6. Packed samples receiving buffers.

The next step is a transformation of polar coordinates into Cartesian ones expressed in the form of offsets, i.e. relative addresses of samples in regard to the origin of memory map of radar searched space.

Main loop of the program executing on DSP 1 is continuously scanning headers of circular buffer slots and starts coordinate transformation procedure when nonempty slot is observed (8). As the transformation is done solely upon data stored in slot header, circular buffer ensures decoupling between processes executing on DSP 0 and DSP 1. The coordinate transformation procedure output consists of two data blocks: the first, which is string of reflectivities and the second, holding coordinates of the points in observed space to which these reflectivities correspond. In general case, reflectivities block is not merely copy of the circular buffer slot, since, in order to avoid empty spots in radar picture appearing in certain modes of work, coordinate transformation routine also executes elaborate filling algorithm which can assign the same reflectivity to neighboring elementary space cells.

After the coordinates transformation, DSP1, by PCI controller in bus master mode, stores block of reflectivity samples ( $v_n$ ) and block of addresses ( $w_n$ ) in one of the six slots,  $v_n$ , of double circular buffer implemented in a common space of host RAM (Fig. 8). After storing, DSP 1 writes length of data blocks to semaphore ( $v$ ), and interrupts host (int  $v$ , Fig. 5). Host interrupt service routine transfers reflectivity data to a memory mapped space through indirect indexed addressing with offsets from address block.

Host processor executing algorithms, described in [13], [8], [7] and [5], performs further processing of radar picture to get meteorological products.

A detailed description of generating meteorological products and hail suppression information system is beyond the scope of this paper and hence is not given here.

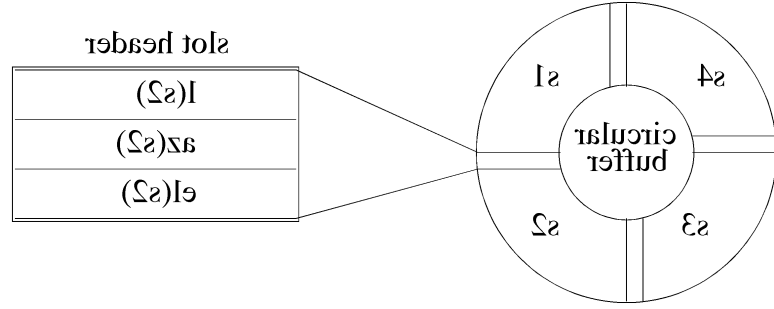


Figure 7. Processed samples circular buffer.

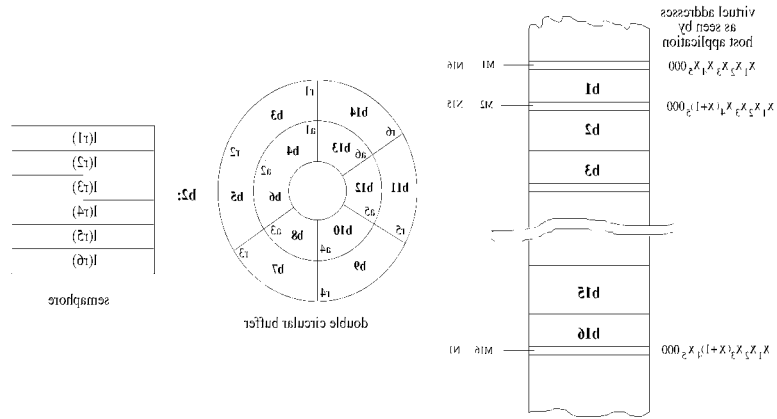


Figure 8. Organization of DSP-host common memory.

Finally, let's give a few concluding remarks on real-time software structure. Host interrupts  $int\ r$  and  $int\ c$  are required by DSP card inability to work as bus master in host I/O address space, and had to be implemented in order to control I/O mapped hardware. The reasons for implementation of host interrupt  $int\ p$  are manifold: 1.) DSP card can address only 32-bit words, and since reflectivity is 8-bit long unacceptable loss of memory space would be incurred, 2.) due to philosophy of PCI, favoring block data transfers, and much simpler programming of DSP card's PCI controller chip when data to be transferred have consecutive addresses, transfer speeds are

much higher for block transfers compared to random memory accesses, 3.) in order to avoid DSP 1 executing physical to virtual addresses conversion, calculated addresses are in offset form and actual addresses conversion is automatically done by host processor's UMM hardware.

Introduction of whole suite of buffers (Figs. 6, 7, 8) although making software much more complex than it theoretically could be, greatly enhances system robustness and prevents data loss due to unpredictable delays incurred mostly by the host operating system running at higher levels of priority, inability of DSP to finish sweep processing by the time next sweep begins, and similar events. Buffering of data also enables DSPs to use the whole intersweep period of 5ms for processing although radar echo lasting time for the maximum distance to be observed by this system  $D_{max} = 250km$ , is  $\tau_{max} = 2D_{max}/c = 1.67ms$ . However, should data loss be inevitable due to prolonged delays, software designs guarantee smooth recovery from any point data and/or synchronization loss can eventually occur.

## 6. Conclusion

The brief description of radar signal and data processing in automated hail suppression system is presented in this paper. Special attention has been paid to the signal processing algorithm whose properties contribute to the quality of generated meteorological products in a direct way. The solution of real-time software structure, calibration of the radar and thresholding process using modified CFAR algorithm are emphasized, as well.

Classical non Doppler weather radar, like MITSUBISHI RC-34A, can measure only one parameter, reflectivity, and they are not enough accurate with possibility of greater probability of operator's wrong rocket launch in decision. Using calibration curves and taking into account all relevant radar parameters, the whole system consisting of radar and automated hail suppression subsystem becomes more accurate and, of course, much faster than manual work. In addition to common tasks, the automated system performs many hail suppression related specialized requirements according to the methods developed in Hydrometeorological Service of Serbia. The system is dedicated to them and is realized by technical solutions as follows:

- tracking and position prediction of a cloud radar echo,
- automatic matched antenna moving pattern and speed according to a selected zoom level,
- zooming,
- moving integration, adaptable, window in range and azimuth domains
- adaptable thresholding for high probability detection purposes,

- making decision about HSS that should launch the rocket with a certain degree of efficiency, and
  - launching rocket elements and timing calculations.
- The initial results of testing of the realized system have lived up to expectations and showed that the system would be supplied with new features increasing efficiency of the whole hail suppression activities.

## REFERENCES

1. I. J. BATMAN: Radar Observation of the Atmosphere. The Univ. of Chicago Press, 1973.
2. J. S. BENDAT, A. G. PIERSON: Measurement and Analysis of Random Data. Wiley, 1968.
3. G. DELLA BRUNA, J. LOSS: Automatic Calibration and Verification of Radar Accuracy for Precipitation Estimation. 27th Int. Conf. on Radar Meteorology, October 1995, Vail, Colorado.
4. M. DIXON, G. WIENER, TITAN: Thunderstorm Identification, Tracking, Analysis, and Nowcasting—A Radar-based Methodology. Journal of Atmospheric and Oceanic Technology, Dec. 1993, Vol. 10, No. 6, pp. 785–797.
5. S. ĐORĐEVIĆ KALAN, B. MILOVANOVIĆ, D. RANČIĆ, A. KOSTIĆ, Z. STANIĆ, I. STOMENOV: Hail Suppression Information System of a Radar Center. Proc. of GIS'95 '95-96, Central Europe, Budapest, 1996, pp. 102–111.
6. R. DOVIK, D. ŽRNIC: Doppler Radar And Weather Observation. 2nd Ed., Academic Press, 1993.
7. P. EFERIĆ, Z. STANKOVIĆ, B. MILOVANOVIĆ, A. KOSTIĆ, V. STANKOVIĆ: System for Digital Processing of Meteorological Radar Images. Proc. of 2nd YU INFO, Brezovica 1996. (in Serbian)
8. P. EFERIĆ, Z. STANKOVIĆ, A. KOSTIĆ: Real Time Software of the Meteorological Radar Images DSP System. Proc. of 3rd YU INFO, Brezovica 1997. (in Serbian)
9. ESP 7: Radar Signal Processor Technical Manual. Enterprise Electronic Corp., March 1996.
10. B. GOLD, C. M. RADER: Digital Processing of Signals. New York, McGraw Hill, 1969.
11. J. J. VAN GORP: Ground Clutter Reduction During Rain Measurements by a Non-coherent Radar System. Weather Radar Networking – Seminar on COST Project 73, 1990, pp. 228–236.
12. HAIL SUPPRESSION CENTER AUTOMATION SYSTEM PROJECT: Faculty of Electronic Eng. Univ. of Niš, December 1995 (in Serbian).
13. A. KOSTIĆ, D. FILIPOVIĆ, N. ĐORĐEVIĆ, D. ĐORĐEVIĆ: Design of Real-time Radar Data Processing Subsystem in Automation System of Radar Center for Hail Suppression. Proc. of 2nd YU INFO, Brezovica 1996. (in Serbian).
14. A. KOSTIĆ, P. EFERIĆ, P. VUKOVIĆ, D. RANČIĆ, Z. STANKOVIĆ: An Approach to Weather Radar Signal Processing by DSP for PC. 3rd International Conference TELSIKS'97, Niš, 1997, pp. 645–648.

20. D. S. ŽRNIĆ: Mean Power Estimation with a Recursive Filter. *IEEE Trans. Aerosp. Electron. Syst.*, Vol. AES-13, May 1977, pp. 281-289.

19. D. S. ŽRNIĆ: Moments of Estimated Input Power for Finite Sample Averages of Radar Receiver Outputs. *IEEE Trans. Aerosp. Electron. Syst.*, Vol. AES-11, January 1975, pp. 109-113.

18. G. B. WALKER, P. S. RAY, D. ŽRNIĆ, R. DOVIK: Time, Angle and Range Averaging of Radar Echoes from Distributed Targets. *Journal of Applied Meteorology*, vol. 19, March 1980, pp. 315-323.

17. H. ROHLING: Radar CFAR Thresholding in Clutter and Multiple Target Situation. *IEEE Trans. Aerosp. Electron. Syst.*, Vol. AES-19, July 1983, pp. 608-621.

16. D. RADINOVIĆ, A. KOSTIĆ: Radar precipitation measurements in Serbia. Research Project of Republic Hydrometeorological Service of Serbia, Beograd, 1997. (in Serbian).

15. B. MILIVOVIĆ, A. KOSTIĆ, V. STANKOVIĆ, N. TRIVUNAC, P. VUKOVIĆ: Design of the Positioning Servo System of the Meteorological Radar MITSUBISHI 34-A. *ETRIAN* 1996. (in Serbian).